Available online at www.sciencedirect.com
SCIENCE DIRECT®
Journal of Power Sources 125 (2004) 183–188
JOURNAL OF POWER SOURCES
www.elsevier.com/locate/jpowsour

Fuel sensitivity tests in tubular solid oxide fuel cells

Srikanth Gopalan [a,*], Gianfranco DiGiuseppe [b]

[a] *Department of Manufacturing Engineering, Boston University, 730 Commonwealth Avenue, Boston, MA 02062, USA*
[b] *Stationary Fuel Cells, Siemens Westinghouse Power Corporation, Pittsburgh, PA 15235, USA*

Received 19 July 2003; accepted 13 August 2003

Abstract

Fuel sensitivity experiments form an important feature of testing solid oxide fuel cell systems. In this paper we describe a fuel sensitivity test and its relation to fuel utilization. The sensitivity of the measured terminal voltage of a tubular solid oxide fuel cell to the fuel utilization provides important information about 'leaks' through the cell. Such leaks could arise from pinholes in the electrolyte or from other sources. First a simple analytical model is presented which is then refined using a numerical simulation. Such tests also provide a methodology to quantify the leaks present in the cell which can ultimately have an effect on fuel cell efficiency.

Keywords: Fuel sensitivity tests; Solid oxide fuel cells; Nernst potential

1. Introduction

Solid oxide fuel cells (SOFCs) are being widely investigated for application in environmentally clean power generation. SOFCs have many important advantages over conventional power generation systems including high efficiency, noiseless operation, modular construction and essentially zero NO_x and SO_x emissions [1,2]. Due to their high efficiencies they also emit a much smaller amount of the greenhouse gas CO_2 compared to conventional power generation systems. Seal-less tubular SOFCs are at the forefront of this technology. In this paper we present an experimental and analytical study of the sensitivity of the tubular SOFC voltage to the fuel utilization. The cell voltage at constant current density has been measured as a function of fuel utilization. It is demonstrated that the observed behavior can be explained using a simple analytical model.

2. Fuel utilization sensitivity experiments

Fuel utilization sensitivity tests are routinely performed on tubular SOFCs. Such tests are used to make a qualitative diagnostic determination of the operational fuel utilization of single cells. In a fuel utilization sensitivity experiment, the cell current (or current density) is held constant and the change in cell voltage is measured as a function of the fuel utilization over a wide range. When the current density is held constant, the total fuel flow to the cell is not constant but is inversely proportional to the fuel utilization. The fuel utilization is defined as the fraction of the input fuel which is electrochemically utilized, i.e. the fuel utilization U is given by the following equation:

$$U = \frac{Q_{\mathrm{ec}}}{Q_{\mathrm{t}}} \tag{1}$$

In the above equation, Q_{ec} (mol/s) is the part of the fuel that is electrochemically utilized in generating electricity and Q_{t} (mol/s) the total fuel input to the cell. The electrochemically utilized fuel can be related to the cell current using Faraday's law as follows:

$$Q_{\mathrm{ec}} = \frac{I}{2F} = \frac{\bar{J}A}{2F} \tag{2}$$

where I is the cell current (A), $\bar{J}$ the average current density (A/cm^2), A the electrode area (cm^2), and F the Faraday's constant (C/mol). It is important to note that in general the current density J in a tubular fuel cell varies as a function of axial position and the current density in Eq. (2) $\bar{J}$ represents a position averaged current density. Fig. 1 shows the geometry of a single cell test article. The terminal voltage of a tubular SOFC is given by the following equation:

$$V_{\mathrm{term}} = V_{\mathrm{Nernst}}(x) - RJ(x) - \eta(x) \tag{3}$$

* Corresponding author. Tel.: +1-617-353-2842; fax: +1-617-353-5548.
E-mail address: sgopalan@bu.edu (S. Gopalan).

0378-7753/$ – see front matter © 2003 Elsevier B.V. All rights reserved.
doi:10.1016/j.jpowsour.2003.08.021

Nomenclature

A	fuel electrode (anode) area (cm^2)
AE/EL	at the cathode (air electrode)–electrolyte interface
D^a_{eff}	effective H_2–H_2O diffusivity in the anode (cm^2/s)
D^c_{eff}	effective N_2–O_2 diffusivity in the cathode (cm^2/s)
EL/FE	at the electrolyte–anode (fuel electrode) interface
F	Faraday constant (96 487 C)
I	cell current (A)
J	current density (mA/cm^2)
K_i	equilibrium constant for H_2–H_2O reaction ($atm^{-0.5}$)
l	total electrochemically active length of tubular SOFC (cm)
$p^{air}_{O_2}$	cathode (air electrode) side oxygen partial pressure (atm)
$p^{fuel}_{O_2}$	anode (fuel electrode) side oxygen partial pressure (atm)
Q	total fuel flow (mol/s)
Q_{ec}	fuel flow which is electrochemically utilized (mol/s)
r	radial position within the cell measured from axis of the tubular SOFC (cm)
R	universal gas constant (8.314 J/(mol K))
R_i	area specific resistance of the tubular SOFC ($\Omega\,cm^2$)
t_a	anode thickness (cm)
t_c	cathode thickness (cm)
U	fuel utilization (0–1)
V_{Nernst}	local Nernst potential (mV)
V_{term}	cell terminal voltage (mV)
x	axial position measured from the fuel inlet point (closed-end) of the tubular SOFC (cm)

Greek letter

η	electrode concentration polarization (mV)

In the above equation, V_{term} is the terminal voltage which is constant and independent of axial position at a given current density and fuel utilization, V_{Nernst} the local Nernst potential at axial position x, R the area specific resistance ($\Omega\,cm^2$) which is independent of position, J the current density which is a function of cell axial position and $\eta(x)$ the sum of various electrode polarization losses at the cathode and anode which is also expected to be a function of cell axial position. It is important to note that the terminal voltage is independent of cell axial position due to the presence of highly conductive axially positioned current collecting bus-bars which act as equipotential surfaces. Taking averages of every term in Eq. (3) the terminal voltage can be written in terms of the

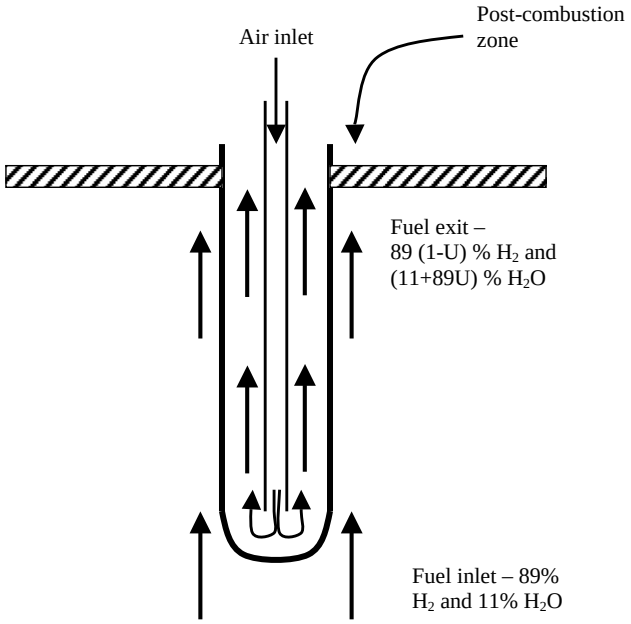

Fig. 1. Schematic of tubular SOFC test article.

average values as follows:

$$V_{term} = \bar{V}_{Nernst} - \bar{J}R - \bar{\eta} \tag{4}$$

The average Nernst potential is the position averaged Nernst potential. In other words

$$\bar{V}_{Nernst} = \frac{1}{l}\int_{x=0}^{x=l} V_{Nernst}(x)\,dx \tag{5}$$

Such an average is necessary since the Nernst potential at a certain axial location along the cell length, under the assumption that the oxygen utilization is negligible, i.e. air is fed to the cell far in excess of the stoichiometrically required amount is given by

$$V_{Nernst}(x) = \frac{RT}{4F}\ln\left[\frac{p^{air}_{O_2}}{p^{fuel}_{O_2}(x)}\right] \tag{6}$$

In the above equation, the partial pressure of oxygen on the airside $p^{air}_{O_2}$ is 0.21 atm and is independent of axial position due to negligible oxygen utilization. On the fuel side the oxygen partial pressure $p^{fuel}_{O_2}(x)$ is determined by the H_2–H_2O equilibrium and is a function of cell axial position. The oxygen partial pressure in the fuel $p^{fuel}_{O_2}$ can then be related to the partial pressure of water vapor and hydrogen on the fuel side $p^{fuel}_{H_2O}(x)$ and $p^{fuel}_{H_2}(x)$, from the H_2–H_2O equilibrium through the following relationship:

$$p^{fuel}_{O_2}(x) = \left(\frac{p^{fuel}_{H_2O}(x)}{p^{fuel}_{H_2}(x)}\right)^2 \frac{1}{{K_i}^2} \tag{7}$$

where K_i is the equilibrium constant for the H_2–H_2O. Henceforth, the superscript fuel will be dropped from $p^{fuel}_{H_2O}(x)$ and

$p_{H_2}^{fuel}(x)$ as these species are present only on the fuel side of the SOFC.

Using Eq. (7) one can write for the oxygen partial pressures in the fuel stream at the fuel inlet and exit points as

$$\ln[p_{O_2}^{fuel}(x=0)] = 2\ln\left[\frac{p_{H_2O}(x=0)}{p_{H_2}(x=0)}\right] - 2\ln(K_i) \quad (8)$$

$$\ln[p_{O_2}^{fuel}(x=L)] = 2\ln\left[\frac{p_{H_2O}(x=L)}{p_{H_2}(x=L)}\right] - 2\ln(K_i) \quad (9)$$

We now make an assumption that the logarithm of oxygen partial pressure on the fuel side is a linear function of axial position. This assumption which is accurate for high average current densities is based on a numerical simulation described later in the paper which predicts that the Nernst potential is linear with cell axial position (see Fig. 3). Under this assumption, the mean $\ln(p_{O_2}^{fuel})$ across the length of the cell is simply given by the arithmetic average of $\ln[p_{O_2}^{fuel}(x=0)]$ and $\ln[p_{O_2}^{fuel}(x=L)]$. Using Eqs. (8) and (9) the average oxygen partial pressure at high average current densities on the fuel side is given by

$$\ln(\bar{p}_{O_2,h}^{fuel}) = \ln\left[\frac{p_{H_2O}(x=0)}{p_{H_2}(x=0)}\right] + \ln\left[\frac{p_{H_2O}(x=L)}{p_{H_2}(x=L)}\right] - 2\ln(K_i) \quad (10)$$

The average Nernst potential at high current densities is then given by

$$\bar{V}_{Nernst,h} = \frac{RT}{4F}\ln\left(\frac{p_{O_2}^{air}}{\bar{p}_{O_2,h}^{fuel}}\right) \quad (11)$$

where $\bar{p}_{O_2,h}^{fuel}$ is given in Eq. (10), where the subscript h stands for high average current density. In the above equation we have assumed that the air side oxygen partial pressure does not change with axial position since the air supplied $p_{O_2}^{air}$ to the cell during these tests is several times (10–15 times) the amount needed for complete stoichiometric oxidation of the fuel.

The water vapor and hydrogen partial pressures in the exit of the fuel cell can be given by

$$p_{H_2O}(x=L) = p_{H_2O}(x=0) + Up_{H_2}(x=0) \quad (12)$$

$$p_{H_2}(x=L) = p_{H_2}(x=0)[1-U] \quad (13)$$

where U is the fuel utilization.

We now assume that the second and third terms in Eq. (4) are independent of fuel utilization. Since the tests are performed at constant average current density and since the ohmic resistance of the cell is not expected to change with fuel utilization neglecting the second term is well justified. However, the third term may well depend on the fuel utilization. Thus this analysis can be regarded as a zeroth order approximation. The effect of fuel utilization on the third term, which represents polarization losses, is explicitly addressed in the numerical simulations presented later in the paper. Under the foregoing assumptions

$$\frac{dV_{term}}{dU} = \frac{dV_{Nernst}}{dU} \quad (14)$$

Substituting Eqs. (10), (12) and (13) in Eq. (11) and differentiating the Nernst potential with respect to the fuel utilization U, and using Eq. (14) we get

$$\frac{dV_{term,h}}{dU} = \frac{dV_{Nernst,h}}{dU} = -\frac{RT}{4F}\left(\frac{1}{(1-U)[p_{H_2O}(x=0) + Up_{H_2}(x=0)]}\right) \quad (15)$$

At low average current densities, a significant length of the cell would be operating close to the exit Nernst potential. In other words, most of the fuel will be consumed very close to the fuel inlet, which is the closed-end of the cell and the Nernst potential would decrease sharply from the inlet value to the exit value within a short length from the inlet. This can indeed be seen in Fig. 3 for an average current density value of 10 mA/cm^2. Thus, the exit Nernst potential, which is strictly a function of fuel utilization at constant temperature, would be attained very close to the closed-end of the cell. Because a very large portion of the cell experiences a Nernst potential close to that of the exit, at a very low average current density, the average Nernst potential can be approximated to that of the exit Nernst potential. In this case the average oxygen partial pressure across the cell, $\bar{p}_{O_2,l}^{fuel}$ (where the subscript l denotes low current density) is given by

$$\ln(\bar{p}_{O_2,l}^{fuel}) = 2\ln\left[\frac{p_{H_2O}(x=L)}{p_{H_2}(x=L)}\right] - 2\ln(K_i) \quad (16)$$

The average Nernst potential in this case is given by

$$\bar{V}_{Nernst,l} = \frac{RT}{4F}\ln\left(\frac{p_{O_2}^{air}}{\bar{p}_{O_2,l}^{fuel}}\right) \quad (17)$$

Substituting Eqs. (12), (13) and (16) in Eq. (17) and using Eq. (14) we get

$$\frac{dV_{term,l}}{dU} = \frac{dV_{Nernst,l}}{dU} = -\frac{RT}{2F}\left(\frac{1}{(1-U)[p_{H_2O}(x=0)+Up_{H_2}(x=0)]}\right) \quad (18)$$

Comparison of Eqs. (15) and (18) reveals that the derivative of the terminal voltage with respect to fuel utilization at low average current density is twice that at high average current densities.

Fig. 2 shows the plots of the absolute values of dV_{term}/dU versus U over a range of fuel utilization values for both low average current density and high average current density cases along with experimentally measured data for average

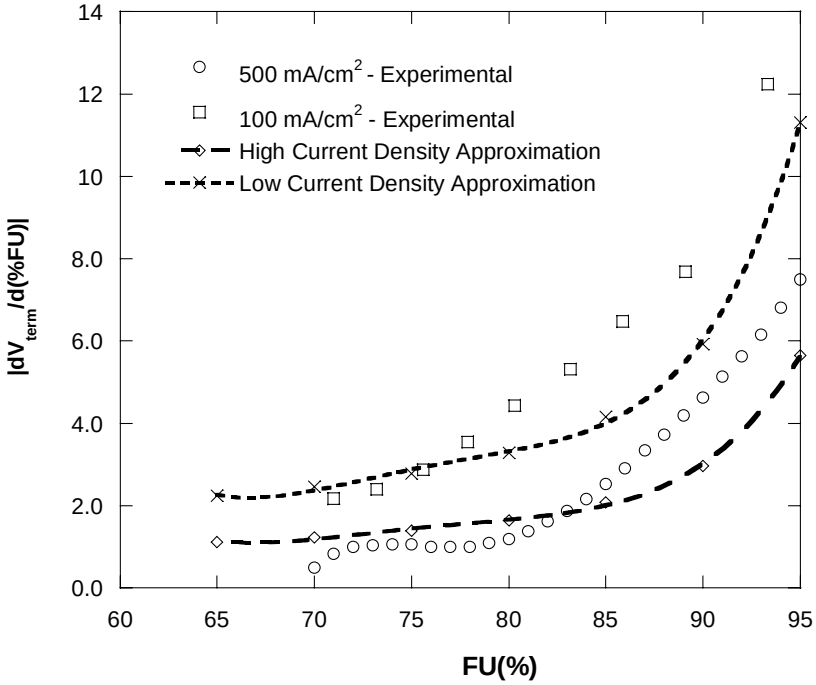

Fig. 2. Fuel utilization sensitivity curves for average current densities of 100 and 500 mA/cm^2 and analytical model predictions.

current densities of 100 and 500 mA/cm^2. As can be seen from Fig. 2, although the experimental data do not match the model developed here perfectly, the overall trend has good qualitative agreement with observed data. Clearly the model needs to be refined to accommodate the effect of ohmic losses and polarization losses to get a more accurate fit to the experimental observations. This is addressed in what follows.

Here we present a refinement to the above model which includes the effect of the second and third terms in Eqs. (3) and (4). Further we show that this modification also allows one to use the fuel sensitivity experiment as a tool to estimate leaks in tubular SOFCs.

The polarization loss $\eta(x)$ is a function of position and is the sum of polarization losses on the air electrode and fuel electrode sides, i.e.

$$\eta(x) = \eta^{\text{air}}(x) + \eta^{\text{fuel}}(x) \tag{19}$$

The air electrode and fuel electrode side polarization losses can in turn be written as:

$$\eta^{\text{air}}(x) = \frac{RT}{4F} \ln\left[\frac{p_{\text{O}_2}^{\text{air}}}{p_{\text{O}_2}^{\text{AE/EL}}(x)}\right] \tag{20a}$$

$$\eta^{\text{fuel}}(x) = \frac{RT}{4F} \ln\left[\frac{p_{\text{O}_2}^{\text{EL/FE}}(x)}{p_{\text{O}_2}^{\text{fuel}}(x)}\right] \tag{20b}$$

The experimental data presented here have been measured at 1000 °C. At this temperature, we have found the charge-transfer polarization losses in our cells are negligible. Thus the polarization losses in Eq. (19) are limited to concentration polarization losses as given in Eqs. (20a) and (20b). The oxygen partial pressures at the electrode/electrolyte interfaces $p_{\text{O}_2}^{\text{AE/EL}}(x)$ and $p_{\text{O}_2}^{\text{EL/FE}}(x)$ can be related to the electrode dimensions and effective binary gas diffusion coefficients as outlined by Kim et al. [3] and Chan et al. [4]. The calculations of Kim et al. [3] and Chan et al. [4] pertain to a planar SOFC with negligible fuel utilization. However, the calculations in the present work are for the case of a tubular SOFC with a large electrode area with practical fuel utilization. The oxygen partial pressure at the cathode–electrolyte interface is determined by relating the oxygen flux J_{O_2} (mol/(cm^2 s)) through the electrolyte to the current density J (A/cm^2), i.e.

$$J_{\text{O}_2} = \frac{J}{4F} = -\frac{D_{\text{eff}}^{\text{c}}}{RT}\frac{\text{d}p_{\text{O}_2}}{\text{d}r} \tag{21}$$

It is important to note that in Eq. (21), the current density (and thus the oxygen flux through the electrolyte), and the radial oxygen partial pressure gradient are a function of cell axial position. Linearizing Eq. (21) we can write

$$J(x) = -\frac{4F}{RT} D_{\text{eff}}^{\text{c}} \frac{p_{\text{O}_2}^{\text{air}} - p_{\text{O}_2}^{\text{AE/EL}}(x)}{t_{\text{c}}} \tag{22}$$

In Eq. (22) $p_{\text{O}_2}^{\text{air}}$ is the oxygen partial pressure in the bulk air stream, $D_{\text{eff}}^{\text{c}}$ the effective binary diffusivity of N_2–O_2 in the gas phase and t_{c} the air electrode thickness. Recognizing that the current density is a function of cell axial position, the interfacial oxygen partial pressure can be obtained from Eq. (22) as follows:

$$p_{\text{O}_2}^{\text{EL/AE}}(x) = p_{\text{O}_2}^{\text{air}} - \frac{RTt_{\text{c}}}{4FD_{\text{eff}}^{\text{c}}}|J(x)| \tag{23}$$

Similarly on the fuel side

$$p_{H_2}^{FE/EL}(x) = p_{H_2}(x) - \frac{RTt_a}{2FD_{eff}^a}|J(x)| \quad (24a)$$

$$p_{H_2O}^{FE/EL}(x) = p_{H_2O}(x) + \frac{RTt_a}{2FD_{eff}^a}|J(x)| \quad (24b)$$

These can then be substituted into Eqs. (20a) and (20b) and the results of the substitution into Eq. (3). This gives the terminal voltage of the cell as a function of the local current density. As defined earlier, the average current density $\bar{J}$ is defined as the total cell current divided by the anode area, i.e. I/A. For a given temperature, fuel utilization and average current density, one can iterate to obtain the current density distribution and the cell terminal voltage. In this calculation the cell is divided into a given number of elements (which can be varied), and at a given average current density, for each of these elements, a local fuel utilization and an elemental current can be defined. The local current density and the local interfacial partial pressures of the various gases can be calculated as a function of cell axial position x through Eqs. (11)–(13). These results can then be substituted in Eqs. (6)–(8) to calculate the Nernst potential and the concentration polarization voltage losses on the cathode and anode sides as a function of cell axial position x. In the calculation, R which is the area specific resistance ($\Omega\,cm^2$) of the cell and the diffusivities D_{eff}^c and D_{eff}^a can be varied to obtain a good fit with the experimentally observed voltage–current density curves (not shown here). Further, the fuel leak from a tubular SOFC can be incorporated in the analysis by including a subtractive term as a variable parameter in the current density in Eqs. (23), (24a) and (24b). This subtractive term is directly proportional to the magnitude of fuel leak.

The Nernst potential as a function of cell axial position calculated using the numerical scheme described above is shown in Fig. 3 for two current densities, 10 mA/cm^2 (low) and 520 mA/cm^2 (high). The dotted line for the 520 mA/cm^2 case represents the linear approximation of the variation of Nernst potential with respect to cell axial position for the high average current density case.

As can be seen from Fig. 3, the assumption of a linear variation in the Nernst potential as a function of axial position in the high average current density case is well justified. Fig. 3 shows the results of the variation of Nernst potential at 520 mA/cm^2 obtained from the numerical simulation and compares it to a straight line fit. Further, the assumption of an average Nernst potential (and therefore logarithm of the fuel side oxygen partial pressure) equal to the exit Nernst potential for the low average current density case is also equally well justified. A subtle point needs to be made here regarding the values of the inlet Nernst potential in the case of high average current density and low average current density cases. From Fig. 3, it is seen that the inlet Nernst potential is ~980 mV for the high average current density case which is close to what should be expected for fuel of composition 89% H_2 and 11% H_2O. However, for the low average current density case it is found to be ~920 mV. At first sight, this is puzzling as the inlet Nernst potentials should be identical if the inlet fuel composition is the same in both

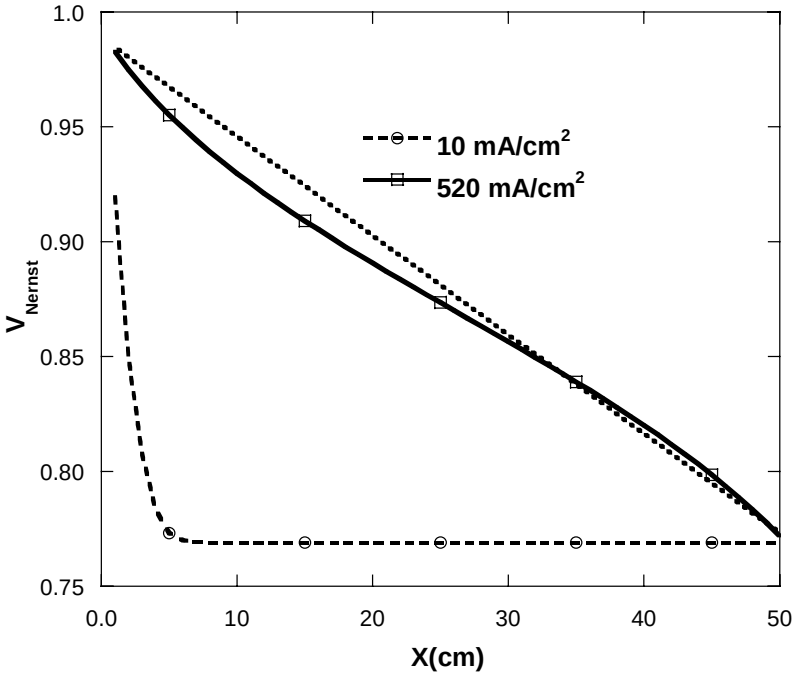

Fig. 3. Plot of Nernst potential as a function of cell axial position from the fuel inlet (i.e. closed-end of cell) at low average current density (10 mA/cm^2) and high average current density (520 mA/cm^2).

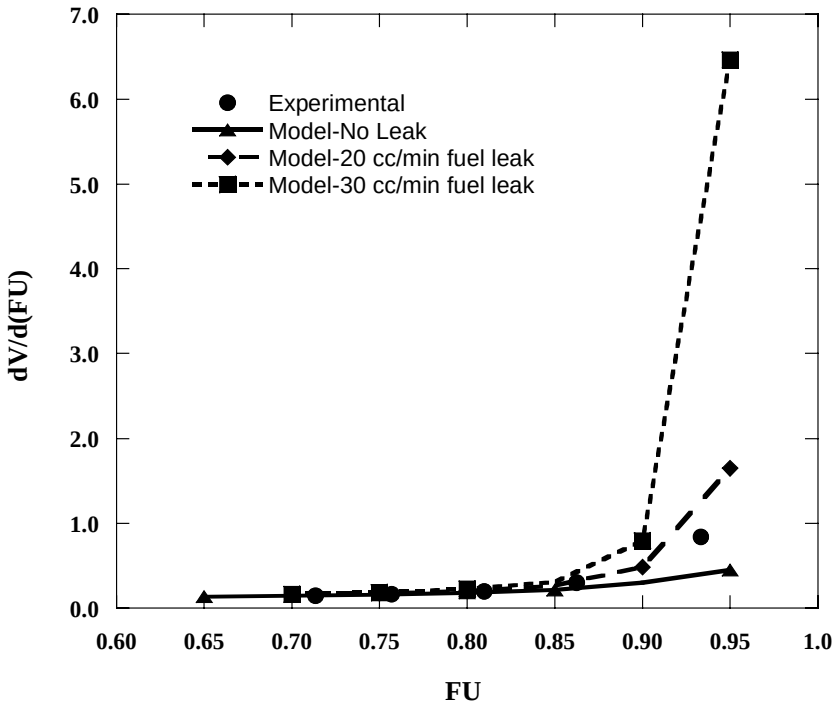

Fig. 4. Experimentally measured fuel utilization sensitivity curves for average current density of 300 mA/cm^2 with overlaid numerical fit for three different leak scenarios.

cases. The answer lies in the fact that the same number of elements (50) was used for both the high average current density and the low average current density cases. However, in the low average current density case, the fuel is utilized very rapidly along the length of the cell. The first data points in both curves do not represent the Nernst potential at the absolute closed-end (which is the fuel inlet point) but an average across the first element. Since the rate of decrease of Nernst potential near the inlet is much more rapid for the low average current density case, the average Nernst potential across the first element for this case is lower. Indeed, if the calculation is repeated with a larger number of elements (200) the first data point increases from 920 to 960 mV for the low average current density case.

Fig. 4 shows the fuel utilization sensitivity, i.e. the first derivative of the terminal voltage of the cell with respect to fuel utilization, versus the fuel utilization for three different fuel leak rates at an average current density of 300 mA/cm^2 along with the experimentally measured data. As can be seen from Fig. 4, the overall trend of these curves is very similar to the curves presented in Fig. 2. Over the course of our experiments it has been found that the threshold value of fuel utilization, i.e. the fuel utilization at which a significant change in the slope of the derivative occurs, is very sensitive to the fuel leak rate of a given cell; higher the leak rate the lower the threshold value of the fuel utilization. In the present instance, a leak rate of 20 cm^3/min fits the measured experimental data very well. Thus, the numerical results presented here in addition to corroborating the main details of the simple analytical model presented earlier can also be used to calculate the leak rates of tubular SOFCs through measurement of the sensitivity of the terminal voltage to the fuel utilization.

3. Conclusions

In the present work, we have provided analytical and numerical calculations to model fuel utilization sensitivity tests on tubular SOFCs. The analytical model has been used to qualitatively explain the shape of the fuel utilization sensitivity curves and the numerical model to quantify fuel leak in tubular SOFCs. The analysis presented here provides the capability to further understand how leaks affect the ultimate performance of tubular SOFCs.

References

[1] S.C. Singhal, in: U. Stimming, S.C. Singhal, H. Tagawa, W. Lehnert (Eds.), Proceedings of the Fifth International Symposium on Solid Oxide Fuel Cells (SOFC-V), vol. 97-18, The Electrochemical Society Inc., 1997, pp. 37–50.
[2] M.C. Williams, in: U. Stimming, S.C. Singhal, H. Tagawa, W. Lehnert (Eds.), Proceedings of the Fifth International Symposium on Solid Oxide Fuel Cells (SOFC-V), vol. 97-18, The Electrochemical Society Inc., 1997, pp. 3–11.
[3] J.-W. Kim, A.V. Virkar, K.-Z. Fung, K. Mehta, S.C. Singhal, J. Electrochem. Soc. 146 (1999) 69.
[4] S.H. Chan, K.A. Khor, Z.T. Xia, J. Power Sources 93 (2001) 130–140.